LIGHTHOUSE

SWEDISH MARITIME COMPETENCE CENTRE

LIGHTHOUSE REPORTS

DEMOPS - Develop Machine learning methods for Operational Performance of Ships

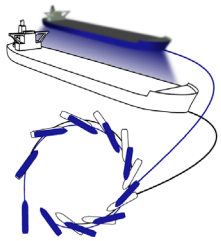

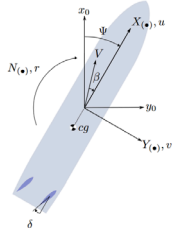

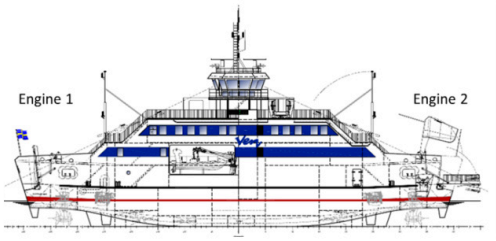

An innovation project carried out within the Swedish Transport Administration's industry program Sustainable Shipping, operated by Lighthouse, published in June 2025

www.lighthouse.nu

LIGHTHOUSE
SWEDISH MARITIME COMPETENCE CENTRE

HÅLLBAR SJÖFART

DEMOPS

- Develop Machine learning methods for Operational Performance of Ships

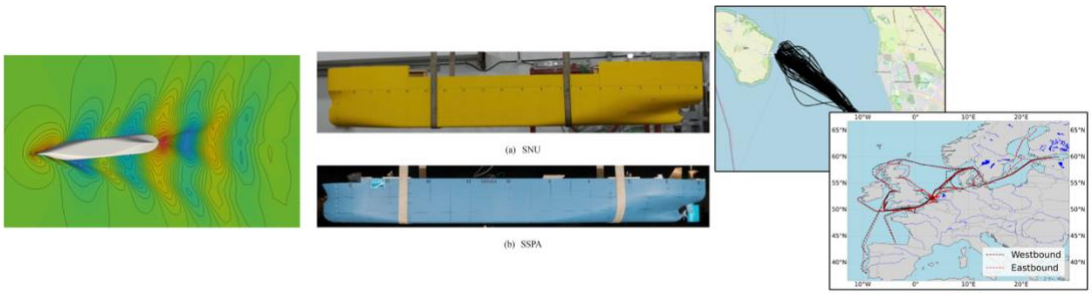

Numerical analysis Experimental tests Full-scale monitoring

Authors

Martin Alexandersson
RISE, SSPA Maritime Center
Wengang Mao
Chalmers University of Technology

In cooperation with
Joakim Moller, Molflow AB
Sofia Werner, RISE, SSPA Maritime Center
Gaute Storhaug, DNV

An innovation project carried out within the Swedish Transport Administration's industry program Sustainable Shipping, operated by Lighthouse

Summary

A ship's fuel consumption can be significantly increased when sailing in harsh sea conditions. Any measures to increase ship energy efficiency must rely on accurate description of the ship's performance. Current theoretical physical models always contain large uncertainties to describe a ship's energy performance especially in the mechanical system models. Some black-box performance models have been constructed by machine learning methods based on ship performance data. But the black box models can be only useful for a specific ship with data inputted for the model construction.

This project first investigates the enhancement of ship manoeuvring models through the integration of prior knowledge embedded in parametric model structures and semiempirical formulas. The study begins with a pre-study focusing on one degree of freedom in ship roll motion, aiming to develop parameter identification techniques and propose a parametric model structure with good generalization. This knowledge is then extended to the manoeuvring problem, with objectives including the development of parameter identification techniques for ship manoeuvring models, proposing a generalizable parametric model structure, mitigating multicollinearity, and identifying added masses. Methodologically, the research employs various parametric model structures for roll motion and manoeuvring, investigated through free running model tests and virtual captive tests (VCT). A novel parameter identification method combining inverse dynamics with an extended Kalman filter (EKF) is proposed. Additionally, a deterministic semi-empirical rudder model is introduced to address multicollinearity issues. The implications of this research suggest that integrating semi-empirical rudder models and utilizing VCT can significantly enhance the accuracy and generalization of ship manoeuvring models, contributing to more reliable and physically accurate simulations in maritime engineering.

Based on the experiences of building various gray-box models for ship dynamics, the knowledge is used to study ship energy performance models with the applications of two case study ships, one on unconventional doubled-ended vessel, and the other on short sea shipping. Based on their data analytics and gray-box models describe those ship's energy performance, a Bayesian based ship voyage planning decision support system was developed during the project. It is demonstrated that the data analysis enhanced decision support system can reduce fuel consumption from 5-10% dependent on the voyages used for those two case study vessels.

Finally, the project leads to a PhD thesis and several scientific publications related to both modelling of ship dynamics and shipping energy efficiency. Numerical simulation analysis data, experimental test data and full-scale measurement data are used in this project to study different choice of modelling techniques.

Sammanfattning

Ett fartygs bränsleförbrukning kan ökas avsevärt när man seglar i tuffa sjöförhållanden. Alla åtgärder för att öka fartygets energieffektivitet måste förlita sig på korrekt beskrivning av fartygets prestanda. Aktuella teoretiska fysiska modeller innehåller alltid stora osäkerheter för att beskriva ett fartygs energiprestanda, särskilt i de mekaniska systemmodellerna. Vissa black-box-prestandamodeller har konstruerats med maskininlärningsmetoder baserade på fartygsprestandadata. Men black box-modellerna kan bara vara användbara för ett specifikt fartyg med data inmatad för modellkonstruktionen.

Detta projekt undersöker först förbättringen av fartygsmanövreringsmodeller genom integrering av förkunskaper inbäddade i parametriska modellstrukturer och semiempiriska formler. Studien inleds med en förstudie med fokus på en frihetsgrad i fartygets rullningsrörelse, med syfte att utveckla parameteridentifieringstekniker och föreslå en parametrisk modellstruktur med god generalisering. Denna kunskap utökas sedan till manövreringsproblemet, med mål som inkluderar utvecklingen av parameteridentifieringstekniker för fartygsmanövreringsmodeller, föreslå en generaliserbar parametrisk modellstruktur, mildra multikollinearitet och identifiera extra massor. Metodologiskt använder forskningen olika parametriska modellstrukturer för rullrörelse och manövrering, undersökta genom frilöpande modelltester och virtuella captive-tester (VCT). En ny metod för parameteridentifiering som kombinerar inversdynamik med ett utökat Kalmanfilter (EKF) föreslås. Dessutom introduceras en deterministisk semi-empirisk rodermodell för att ta itu med multikollinearitetsproblem. Implikationerna av denna forskning tyder på att integrering av semi-empiriska rodermodeller och användning av VCT avsevärt kan förbättra noggrannheten och generaliseringen av fartygsmanövreringsmodeller, vilket bidrar till mer tillförlitliga och fysiskt exakta simuleringar inom sjöfartsteknik.

Baserat på erfarenheterna av att bygga olika grå-box-modeller för fartygsdynamik, används kunskapen för att studera fartygs energiprestandamodeller med tillämpningar av två fallstudiefartyg, ett på okonventionella dubbelsidiga fartyg och det andra på närsjöfart. Baserat på deras dataanalys och grå-box-modeller beskriver dessa fartygs energiprestanda, utvecklades ett Bayesianskt baserat beslutsstödssystem för fartygsresaplanering under projektet. Det har visat sig att det förbättrade beslutsstödssystemet för dataanalys kan minska bränsleförbrukningen från 5-10% beroende på de resor som används för dessa två fallstudiefartyg.

Slutligen leder projektet till en doktorsavhandling och flera vetenskapliga publikationer relaterade till både modellering av fartygsdynamik och sjöfartens energieffektivitet. Numeriska simuleringsanalysdata, experimentella testdata och fullskaliga mätdata används i detta projekt för att studera olika val av modelleringstekniker.

Contents

1 Introduction

There are many scenarios where constructing a model of a ship is beneficial. For instance, a digital twin is a kind of dynamic model as a real-time digital replica of a physical ship. It continuously receives data from its physical counterpart through sensors. The concept originated from NASA's efforts to improve the physical-model simulation of spacecraft. Today, digital twins are used in many industries, including manufacturing, urban planning, healthcare, and more. They help organizations simulate real-world scenarios and make better decisions by providing real-time data and insights. A virtual prototype is like the digital twin model but primarily used for simulation and testing during the design phase. It does not necessarily receive real-time data from a physical counterpart – so it can be used before the real ship exists.

The fundamental concept of a model is to predict outcomes that might be too dangerous, difficult, or costly to test with an actual ship. For instance, when evaluating millions of alternative scenarios during optimization, a cost-efficient model is crucial. Building a model before constructing the real ship is a prudent approach, like how an architect creates a model of a house before construction Fig.1.1. Scale model testing at facilities such as the RISE SSPA Maritime Center is often conducted before ships are built to investigate ship dynamics. However, this process is costly and time-consuming, and the facilities have inherent physical constraints that may limit the comprehensive study of ship dynamics.

Figure 1.1 RISE SSPA Maritime Center.

Instead, a more theoretical approach is adopted. Computational fluid dynamics (CFD) describes the hydrodynamics of ships based on fundamental physics principles. However, there are many situations where CFD is not feasible. The calculations might be too expensive, or the geometries, calculation domain, or boundary conditions might not be defined with sufficient accuracy. Therefore, in many situations, we must accept the lack of a complete physical understanding of the system and instead use a data-driven model that mimics the system's behaviour from observations. This project has investigated such data-driven models. Appropriate mathematical model structures to describe the underlying physics have been established, and methods to identify them from either CFD calculations or recorded ship trajectories have been proposed.

The term “model” is frequently used in this report, but it carries different meanings across various engineering disciplines. To avoid confusion, this report adopts a more precise definition by distinguishing between “model structure” – defined for mathematical models

by "model equations" – and "identified model", which refers to the complete model, including the identified parameters within the model equations.

Model structures are often categorized in the literature as either parametric models (Fig.1.2) or non-parametric models (Fig.1.3). A third category, hybrid models, combines parametric models with non-parametric models. The following definitions have therefore been adopted in this project: if the model structure is defined by explicit mathematical formulas that have parameters in it, it is categorized as a parametric model; all other model structures are categorized as either non-parametric or hybrid models.

$$X'_H = X'_0 + X'_{rr}r'^2 + X'_u u' + X'_{vr}r'v' + X'_{vv}v'^2$$

$$Y'_H = Y'_0 + Y'_{rrr}r'^3 + Y'_r r' + Y'_{vrr}r'^2 v' + Y'_{vvr}r'v'^2 + Y'_{vvv}v'^3 + Y'_v v'$$

$$N'_H = N'_0 + N'_{rrr}r'^3 + N'_r r' + N'_{vrr}r'^2 v' + N'_{vvr}r'v'^2 + N'_{vvv}v'^3 + N'_v v'$$

Figure 1.2, Example of a parametric model.

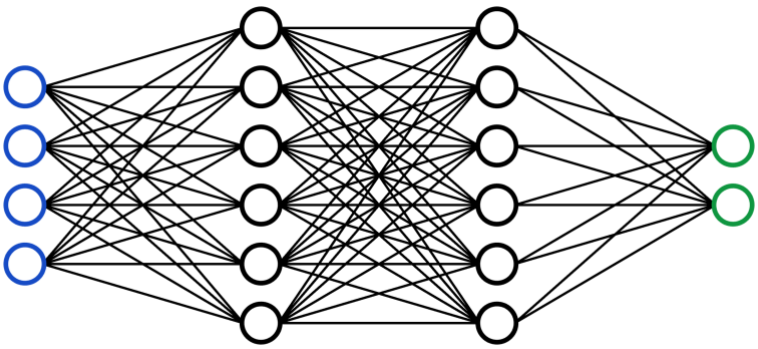

Figure 1.3, Example of a non-parametric model.

Multicollinearity refers to a situation in statistical modelling where two or more predictor variables are highly correlated, making it difficult to isolate the individual effects of each predictor on the dependent variable. An example is when the ship has a drift angle so that the total side force Y acting on the ship from the oblique flow generates lift forces on both the hull Y_H and the rudder Y_R, as shown in Fig.1.4. The hull force and rudder force will be highly correlated in this situation, and it will be hard to identify their individual contributions when only the total force is measured. This issue is particularly relevant in the field of ship modelling, where numerous hydrodynamic coefficients and parameters are involved. The higher correlations of parameters are, or the stronger multicollinearity exists, the more difficult it is to identify regression coefficients separately (Yoon and Rhee, 2003). Yaw rate and drift angle are correlated during manoeuvres, as shown in Fig.1.5, which makes it difficult to separate their influences. The best option to mitigate multicollinearity is to get more informative data with persistence of excitation including conditions where the input signals used in system identification are sufficiently rich in frequency content to excite all the modes of the system. This ensures that the system's response contains enough information to uniquely identify the system parameters. Without persistence of excitation, the identified model may not accurately represent the ship's behavior in all scenarios. For instance, even though there might be millions of datapoints available, if nothing has happened for a long time, the data is not very informative and cannot be used to identify a model.

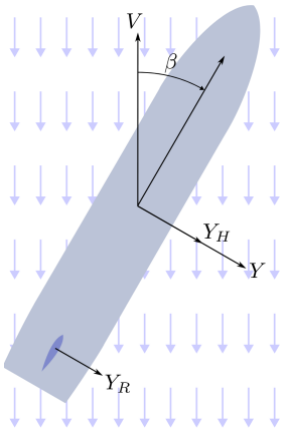

Figure 1.4, Multicollinearity between hull and rudder forces.

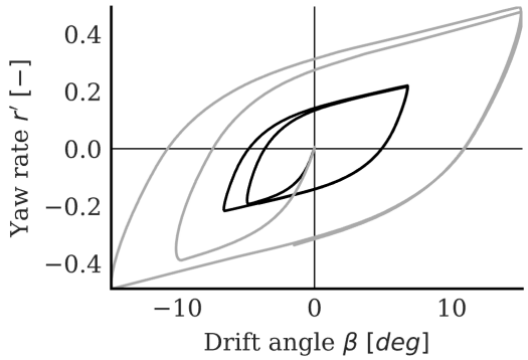

Figure 1.5, Yaw rate and drift angle are correlated during zigzag manoeuvring tests.

1.1 Motivation and objectives

System identifications of parametric models has been conducted since the late 1970s from free running tests, and for even longer times from captive tests. The first papers about non-parametric models were published in the late 1990s, with an increasing popularity during the past 15 years, especially within the field of autonomous vessels. Today there are still papers being published about both these approaches, so there seems to be no consensus which one is the better. Further progress within machine learning can be expected within the coming years, with a bright future for the non-parametric models and the hybrid approaches. The lack of informative data and persistence of excitation will however remain a big challenge.

One aspect of indirect informative data that is often overlooked is the prior knowledge about ship hydrodynamics from previous experimental works and other physical insights. This indirect informative data is often embedded in the parametric model structures, which parameters should be included or excluded from a model have often been chosen with careful consideration from experimental works or physical reasoning. There are also semi-empirical formulas in the literature that could potentially be used to add more informative data. This is a subject that needs further investigation, and the research question of this project has therefore been formulated in the following way:

- How should prior knowledge embedded in parametric model structures and semiempirical formulas be used to enhance the generalization of ship models?
- How can the models/knowledge be utilized to increase shipping energy efficiency?

To provide a clear path through this research, the research questions have been broken down into the following work tasks/subjects, including develop parameter identification techniques for roll motion models with good generalization based on prior knowledge from model tests, develop parameter identification techniques for ship manoeuvring models by applying different data analytics and machine learning modelling techniques to investigate the problems of multicollinearity, generalization and integration of semiempirical formulas for data-driven models, as well as what decision support system to be combined with maritime data analytics and machine learning modelling to increase shipping energy efficiency.

1.2 Assumptions and limitations

For the first part of the project, i.e., to create physics-informed models for ship dynamics, the ship's dynamics are described by the motion of the ship and the forces that cause this motion. Modelling of the ship dynamics for a ship at sea is a very complex task that involves large uncertainties regarding the environmental conditions from the wave, winds and currents. The ship's dynamics has therefore been studied in calm water conditions, as a simplification in this project. This addresses the manoeuvring performance of the ship, where the calm water dynamics can be studied in isolation from the remaining components at sea.

Since a ship's dynamics is closely related to the energy consumption and controllability of the ship, data analytics and machine learning are used to demonstrate their applications to increase shipping energy efficiency. In this project, only two case study ships, i.e., one double ended vessel, and one short sea shipping vessel, are used in this study. Weather conditions are assumed to be known for the decision support of energy efficient ship operations.

2 Model structures of ship dynamics

The model structures in this project are expressed as memory-less state space models, following the Markov process assumption. This assumption implies that the forces acting on the ship at each time instant depend only on the current state – so that previous events do not affect the current state. The state space model can therefore express the change of state $\dot{\boldsymbol{x}}$ from the current state vector $\boldsymbol{x}$ and the input vector $\boldsymbol{u}$ through the transition function $f(\boldsymbol{x}, \boldsymbol{u})$:

$$\dot{x} = f(x, u)$$

The change of state, estimated by the transition function, can be used to simulate the ship motions with time integration. The position and orientation, velocities and turning rate defines the state of the ship in three degrees of freedom $\boldsymbol{x} = [x_0, y_0, \Psi, u, v, r]^T$ as shown in Fig. 2.1. The ship kinematics can be expressed as function of a velocity vector $\boldsymbol{v} = [u \quad v \quad r]^T$.

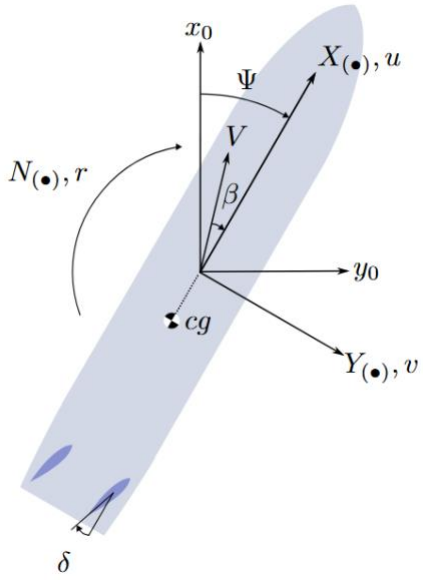

Figure 2.1, Relations between the earth fixed and ship fixed reference frames, showing the velocities and forced in the ship fixed frame.

The ship acceleration $\dot{\boldsymbol{\upsilon}}$ is expressed with the inverse mass matrix $\boldsymbol{M^{-1}}$ and force vector $\boldsymbol{F}$ through the equation of motion.

$$\dot{\boldsymbol{\upsilon}} = \mathbf{M^{-1}F}$$

The ship acceleration vector $\dot{\boldsymbol{\upsilon}}$ can be used together with the global velocities $\dot{x_0}$, $\dot{y_0}$, and r to form the transition function.

$$f(\boldsymbol{x}, \boldsymbol{u}) = [\dot{x_0}, \dot{y_0}, \mathrm{r}, \dot{\boldsymbol{\upsilon}}]^T$$

The system identification can now be split into the problem of determine the mass matrix $\boldsymbol{M}$ and the problem to determine a parametric model of the forces $\mathbf{F}$ acting on the ship as explained in the next section.

2.1 Parameter identification

The rigid body part of the mass matrix was determined by swing tests in air and the added masses were determined with potential flow calculations. In this project, the force models were identified from either captive test (CT) or the free-running test (FT). Captive model tests (CMT) are the classical way of conducting captive tests, which can be performed in various ways: with an XY-carriage, rotating arm, or planar motion mechanism (PMM). CT can also be performed with CFD in virtual captive tests (VCT). FT data are collected from either model tests full-scale tests, or operational data. CT data is generally more applicable in virtual prototyping when assessing the manoeuvring performance before ships are built. FT data, on the other hand, are generally more applicable for existing ships, in a digital twin context.

2.2 System identification from captive tests

Because of the Markov assumption, the force model m can be expressed as a function surface of the input velocities, rudder angle δ, and the propeller thrust T.

$$F = [X_D, Y_D, N_D]^T = m(u, v, r, \delta, T)$$

The inputs are varied during the captive tests to identify the function surface as shown in Fig. 2.2. The function surface is assumed to be expressible with a predefined model structure, containing a set of polynomials to express the forces. There are a many such mathematical models proposed in the literature (Abkowitz, 1964; Nomoto et al., 1957; Norrbin, 1971; Yasukawa and Yoshimura, 2015). The data from the captive tests is used to identify the parameters within the mathematical force model with linear regression.

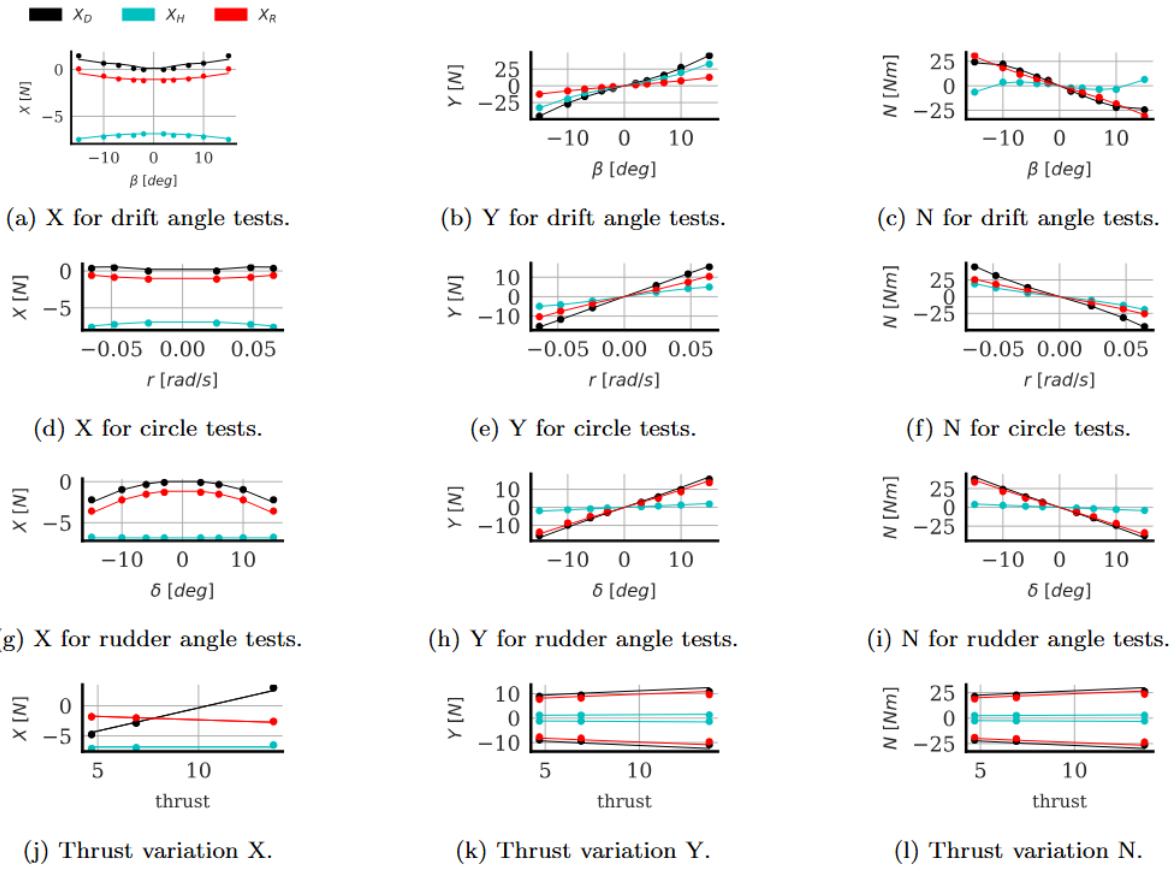

(a) X for drift angle tests. (b) Y for drift angle tests. (c) N for drift angle tests.

(d) X for circle tests. (e) Y for circle tests. (f) N for circle tests.

(g) X for rudder angle tests. (h) Y for rudder angle tests. (i) N for rudder angle tests.

(j) Thrust variation X. (k) Thrust variation Y. (l) Thrust variation N.

Figure 2.2, Forces obtained from captive tests.

2.3 System identification from free running tests

Unlike the captive test, free running test cannot measure the forces directly. The forces were instead estimated by using the equation of motion to calculate the inverse dynamics.

$$\mathbf{F} = \mathbf{M}\dot{\boldsymbol{\nu}}$$

The acceleration vector $\dot{\boldsymbol{\nu}}$ was estimated by an extended Kalman filter. An example of the inverse dynamics forces is shown in Fig. 2.3, where the forces during a turning circle manoeuvre have been estimated. The estimated forces can be used to identify a force model in a similar way as the captive test, which is referred to as inverse dynamics regression.

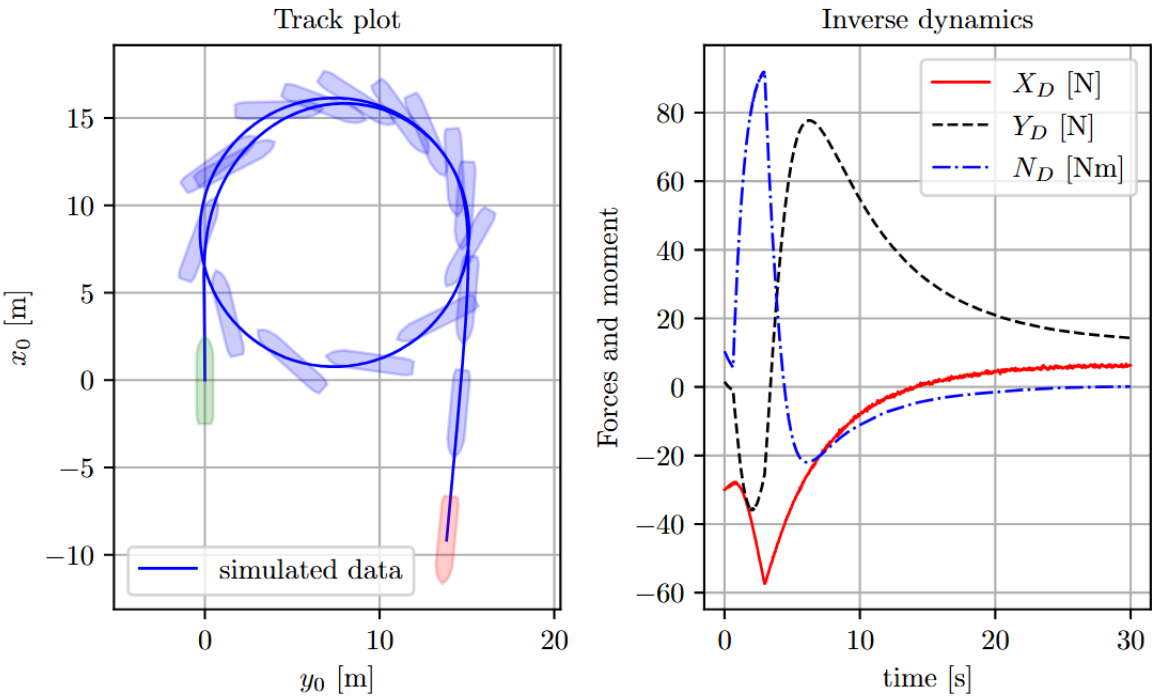

Figure 2.3. Forces and moments calculated by inverse dynamics on data from a turning circle test.

3 Model structure for ship power performance model

A ship's energy performance model is necessary to evaluate the energy costs in any energy efficiency shipping measures. The general procedure for such a ship energy performance model, i.e., predict ship speed from marine engine power, or predict engine power from ship speed, can be estimated physically as presented in in Fig.3.1.

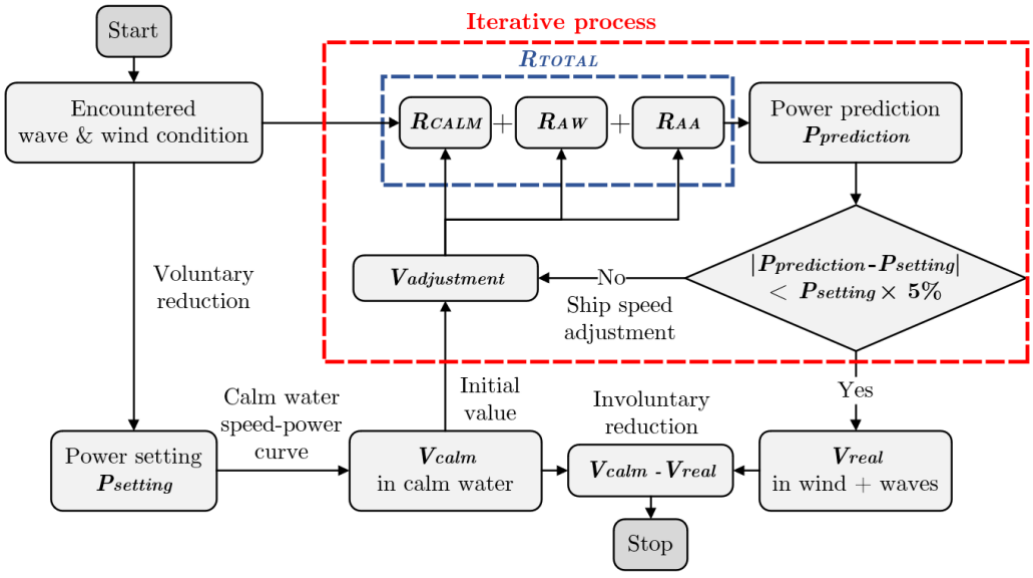

Figure 3.1. A general ship energy consumption estimation process.

Based on the ship's speed through water V, by combining the ship's characteristics and the encountered sea conditions, the total resistance R_{Total} is first obtained. The propulsion power Ps can then be calculated based on the effective power from propeller against the resistance R_{Total}, engine configurations, and propeller efficiencies. And in the end, the fuel

cost *Fc* is obtained based on *Ps* and Specific Fuel Oil Consumption (SFOC), representing the efficiency of the ship engine. The following relationships between *Fc*, *Ps* and SFOC generally applies:

$$F_c = P_s \times SFOC$$

where *SFOC* represents the efficiency of the engine, and its value varies under different speeds or propulsion power. In the industry, the data of SFOC is calibrated through a series of engine testing, and the curve of SFOC with respect to the propulsion power *Ps* is derived by data analyses. The theoretical SFOC curve indicates the average SFOC within the measured time interval, but discrepancies could remain between the measured SFOC, and the theoretical values from manufacturers. Figure 3.2 shows an example of SFOC measurement data. Its accuracy can therefore be improved through better modelling of SFOC under various operational conditions. Due to the hull-propulsion-engine coupling, the efficiencies of the engine, i.e. SFOC, are also significant for the final energy cost.

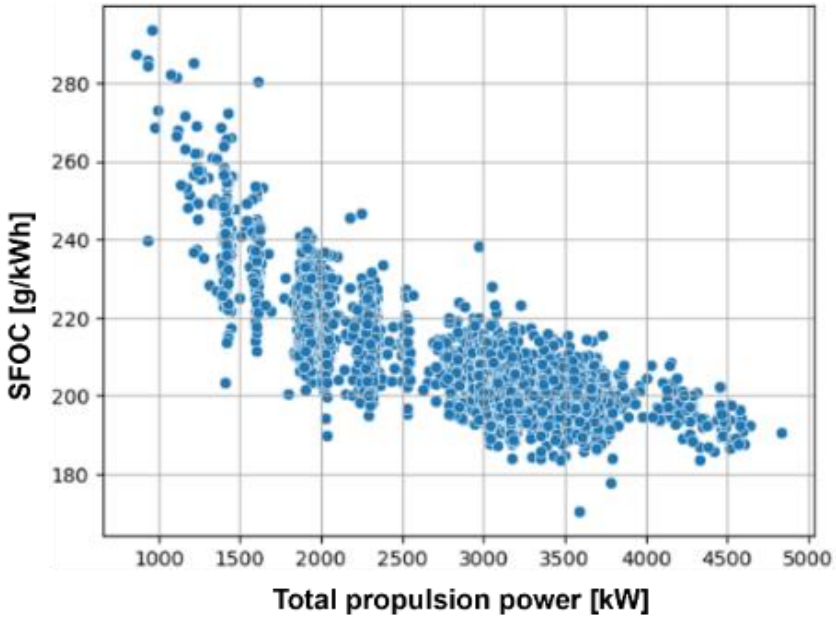

Figure 3.2. The measurement data of SFOC under different propulsion powers.

Both power and fuel consumption could be modelled in various ways from exiting research, such as empirical (Lang & Mao, 2020, 2021) and more advanced machine learning approaches (Lang et al., 2022, 2024). Additionally, SFOC varies under actual operational conditions, also potentially causing discrepancies in fuel estimation and affecting voyage optimization. Further investigation is needed to understand how they influence decision support system for shipping energy efficiency. Depends on how much prior-knowledge/physical principle and the volume of ship performance monitoring data are available to build models estimating the power and fuel consumption, different modelling techniques can be categorized into black-box, white-box and grey-box models as show in Fig.3.3. In the following subsections, some basic introduction about those models, especially the semi-empirical models are presented. More detailed information can be referred to the listed scientific publications.

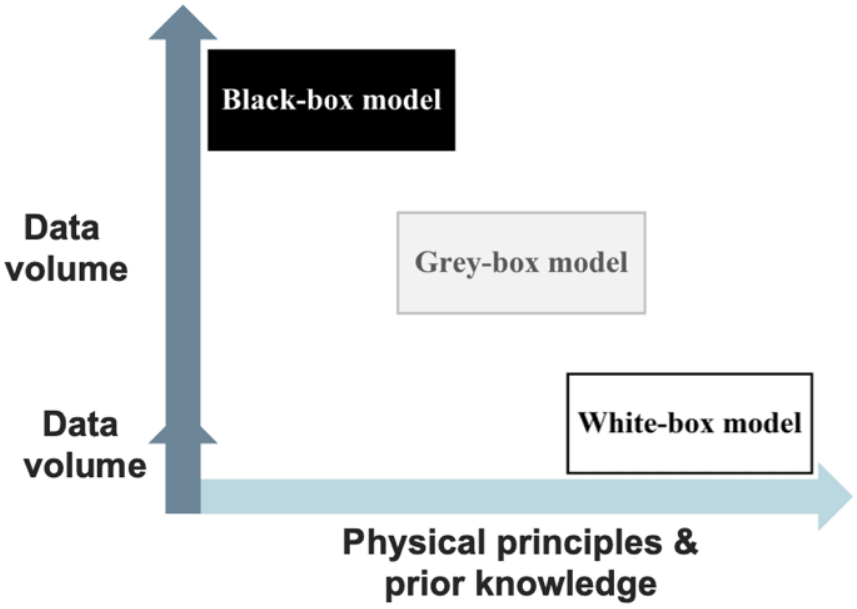

Figure 3.3. Different performance models used for the cost function

3.1 Speed-power empirical model

Since the shaft power directly relates to the total work done by the engine, the first cost function aims to optimize the overall sailing cost by minimizing the shaft power, i.e., include a speed-power relationship. In this part, the ship performance model is developed by a conventional empirical approach as shown in Fig.3.1. From the speed over ground V_g, we first need to determine the ship's speed through water V and the speed of ocean current V_c.

$$V = V_g + V_c$$

Then based on the encountered sea condition, and the ship's characteristics, the total resistance R_{Total} is derived from adding calm water resistance R_{Calm}, added wind resistances R_{Wind}, wave R_{Wave}, current R_C, and shallow water R_S, as follows:

$$R_{Total} = R_{Calm} + R_{Wind} + R_{Wave} + R_C + R_S$$

The above forces are calculated based on (Lang & Mao, 2020, 2021) in this part. The total resistance R_{Total} is counteracted by the effective power of engine and propellers to propel the ship forward, under the speed through water V. And this effective power is the shaft power Ps taking into account the efficiency and manufacturer specifications. The shaft power Ps can be derived as follows:

$$P_s = R_{Total} * \eta$$

η is the overall efficiency coefficient that calculated based on (Holtrop & Mennen, 1982). It includes the hull efficiency, propeller open water efficiency, and engine shaft efficiency. And eventually, the relationship between the speed through water V to the shaft power Ps is established.

3.2 The semi-empirical model for added resistance in waves

The accuracy of a ship's resistance and propulsion calculation is vital for the entire iterative process. First, a further improved semi-empirical model for added resistance due to head regular waves is presented. Then, extension formulas are proposed to consider effect of other wave headings. Finally, a correction factor is proposed in the component of added resistance to consider nonlinear effect of power consumption in large sea states. Then R_{TOTAL} is estimated by:

$$R_{TOTAL} = R_{CALM} + R_{AA} + R_{AW}$$

where R_{CALM} and the propulsive efficiency η_D can be quite accurately estimated by model test results in this study, and R_{AA} is estimated by the well-established method in ISO (2015). The preliminary correction factor is found and tuned by analyzing the difference between conventional prediction and full-scale measurements used in this study. For a general application of this correction factor, comprehensive investigation should be conducted to establish such a flexible formula/factor, based on more extensive experimental tests and full-scale measurements. While different components in the proposed model for R_{AW} are further verified and validated in the following analysis.

For a ship sailing in head waves with speed V and $\beta = 0$, the added resistance in regular waves of frequency ω can be evaluated by the sum of two components, i.e., added resistance due to wave reflection R_{awr}, and due to ship motions R_{awm} as (Strom-Tejsen et al. 1973):

$$R_{aw}(\omega|V,\beta) = R_{awr}(\omega|V,\beta) + R_{awm}(\omega|V,\beta)$$

For the semi-empirical models of added resistance in head waves, all the detailed formulas are given in Lang and Mao (2020) for head waves and Lang and Mao (2022) for arbitrary waves.

An actual sea state is often described by a wave spectrum of predefined formats multiplied by a spreading function $D(\theta)$. In this study, the JONSWAP wave spectrum and a Consine-Squared spreading function $D(\theta)$, in terms of the significant wave height H_s, wave peak period T_p, peakedness factor γ and the wave spreading direction θ, are applied to describe irregular waves of a ship's actual sailing wave conditions,

$$S(\omega|H_s,T_p,\gamma)D(\theta) = \frac{320{H_s}^2}{{T_p}^4\omega^5}\exp\left(\frac{-1950}{{T_p}^4\omega^4}\right)\gamma^{\exp\left[\frac{-(\omega-\omega_p)^2}{2\sigma^2\omega_p^2}\right]}D(\theta)$$

$$D(\theta) = \begin{cases}\frac{2}{\pi}\cos^2(\theta) & \text{if } -\frac{\pi}{2} \le \theta \le \frac{\pi}{2} \\ 0 & \text{otherwise}\end{cases}$$

where γ is set to the standard value 3.3, and the spectral width parameters $\sigma = 0.07$ for $\omega \le \omega_p$, $\sigma = 0.09$ when $\omega > \omega_p$. The added resistance in waves R_{AW} under

actual wave environments (irregular waves) is conventionally estimated by:

$$R_{AW}(\omega|H_s,T_p,\gamma,V,\beta) = 2\int_0^{\infty}\int_{-\frac{\pi}{2}}^{+\frac{\pi}{2}} S(\omega|H_s,T_p,\gamma)\frac{R_{aw}(\omega|V,\beta)}{\zeta_a(\omega)^2}D(\theta-\beta)d\theta d\omega$$

where $\zeta_a(\omega)$ is amplitude of the regular wave to get the added resistance $R_{aw}(\omega)$. The term R_{aw}/ζ_a^2 is often referred as the transfer function of ship resistance.

3.3 Speed-power machine learning model

Recent research and industry advancements have led to the development of machine learning models, which can effectively predict ship performance under varying conditions. Various machine learning techniques have been applied to describe the speed-power relationship of ships in the existing research.

Different models are developed and compared to identify the method with the least discrepancy for ship performance modeling in (Lang et al., 2021). It can be seen in Fig. 3.4 that, the XGBoost technique demonstrates a cumulative discrepancy of no more than 3% in power prediction over more than 10 days of actual sailing. In contrast, other methods such as neural networks, support vector regression, generalized additive models, and statistical polynomial regression show discrepancies of around 20%-30%.

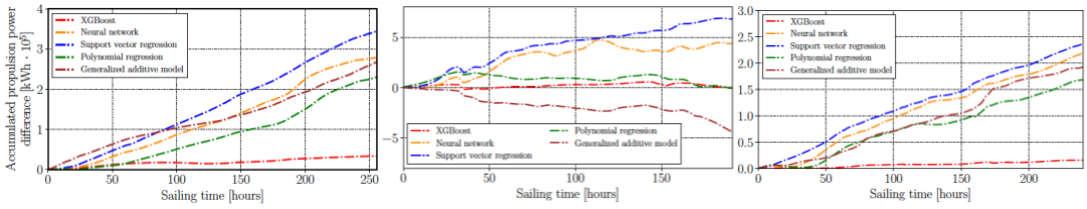

(a) Voyage 1 (b) Voyage 2 (c) Voyage 3

Figure 3.4. The discrepancies in propulsion power using different machine learning models.

3.4 Optimization framework in DSS for shipping energy efficiency

The flowchart and methods for the proposed DSS of double-ended ferries are presented in Fig. 3.5 to determine optimal operational set-point parameters/inputs of a specific trip, i.e., an input layer of all necessary information about the trip, data-driven models required to describe the ship and engine performance, and Bayesian optimization algorithm with prior belief from proper/historical trip settings. For the DSS working onboard, the optimization algorithm (e.g., Wang et al. 2019, Chen and Mao 2024) integrated should be computational efficient. The Bayesian algorithm that can utilize prior sailing experiences/data is proposed to fulfil such requirements.

First, the input layer of the DSS includes both prior, current, and forecast information related to the specific trip for its DSS. They serve as the interface and fed into the decision-making model as in Fig.3.5.

- *Reference route.* It provides historical sailing waypoints (longitudes, latitudes, heading angles, etc.) like this trip, as well as speed V_g and fuel consumption.

- *MetOcean data.* It is extracted from weather forecasting database. Once the route coordinates are set, and the trip schedule is known the data is interpolated to match the position and times.
- *An initial guess or prior of "pre-assumed" optimal operation parameters.* This optimization initialization guides the optimizer into a search space that is most likely to contain stationary points that allow for the reduction of fuel consumption.

For optimal navigation of such double-ended ferries, one of the big challenges is to understand the ferry's performance in terms of different engine settings. Reliable models are rarely available, and there are not mature enough guidelines to assist actual navigation of those ferries. As the increase of shipping digitalization, some data collection systems can be easily installed onboard those ferries to assist development of the DSS for energy efficient operations. In the following, a case study double-ended ferry with data collections onboard is used to demonstrate the challenges and validate the proposed DSS.

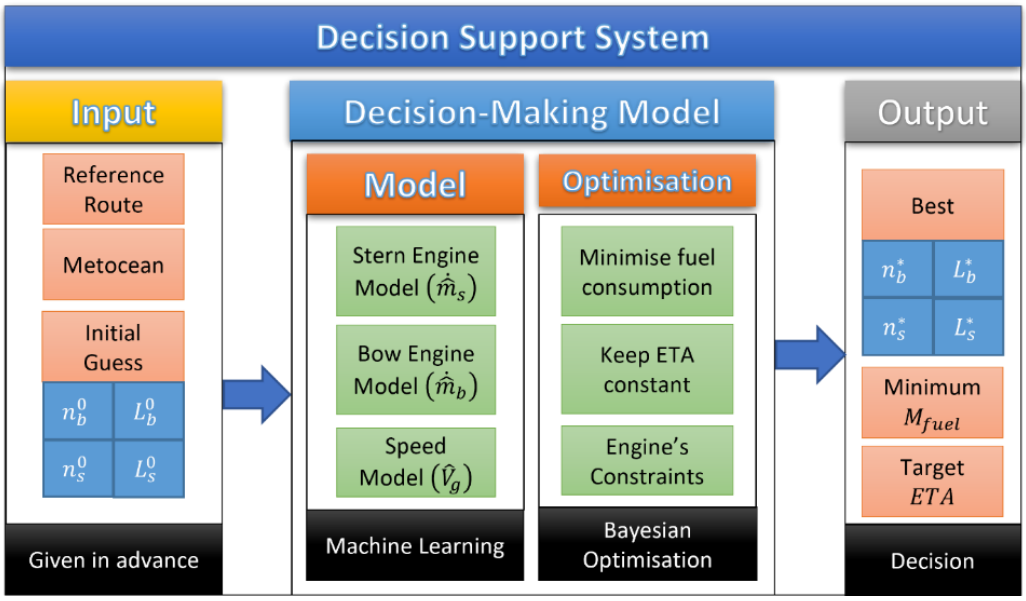

Figure 3.5. The flowchart and methods of the proposed Decision Support System (DSS).

4 Results for ship dynamics

The initial step in this research project was to simplify the system identification of the ship dynamics to a single degree of freedom, specifically the roll motion. The important findings from this initial simplification are summarized below followed by the results from the subsequent research where the system identification was expanded to three degrees of freedom manoeuvring. The research results for ship dynamics using experimental tests and some CFD simulations for modelling purposes are summarized in this Trafikverket/Lighthouse funded PhD thesis (Alexandersson 2025), which is composed scientific publications of Alexandersson et al.(2021, 2022, 2023, 2024), as well as an extra submitted journal publication.

4.1 Roll motion

The objective was to develop parameter identification techniques for roll motion models derived from roll decay model tests. The roll damping was studied using time series data from 250 roll decay tests assembled by RISE at the Maritime Dynamics Laboratory, SSPA Maritime Center. Additionally, the aim was to propose a parametric model structure for roll motion dynamics that generalizes well, based on prior knowledge from the model tests. System identification was conducted on linear, quadratic, and cubic models. Results from the simulations with the identified models (from one of the roll-decay tests) are presented in Fig. 4.1. The cubic and quadratic models reproduced the model test well, but the linear model was too simple to provide an accurate representation for both smaller and larger roll angles. The amplitude decrement Φ_a and roll damping B for each oscillation can be visualized, as seen in Fig. 4.2. The quadratic model, with fewer parameters than the cubic model, is expected to have a higher level of generalization at the same accuracy and was therefore selected as the best mathematical model for the roll motion.

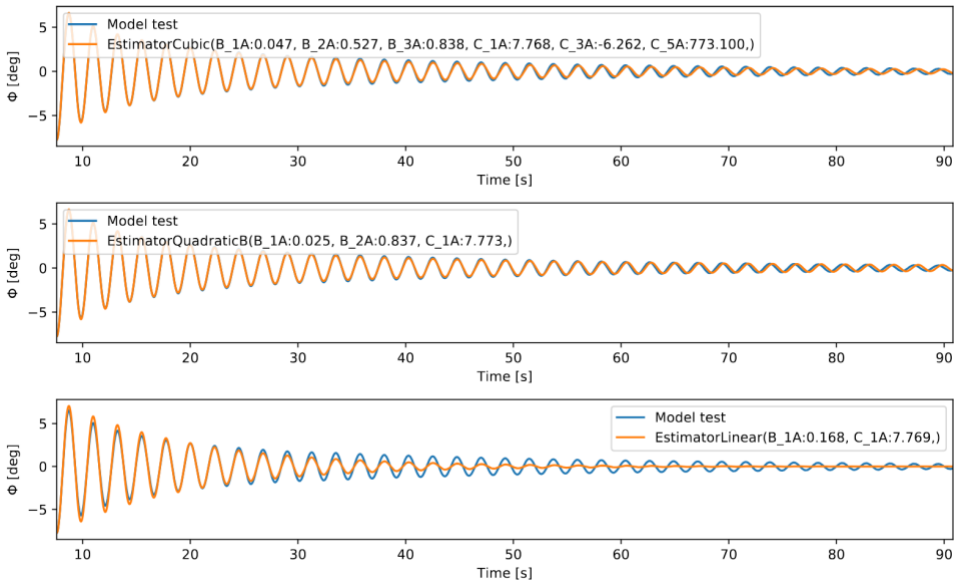

Figure 4.1. Roll decay estimation with identified cubic, quadratic, and linear models.

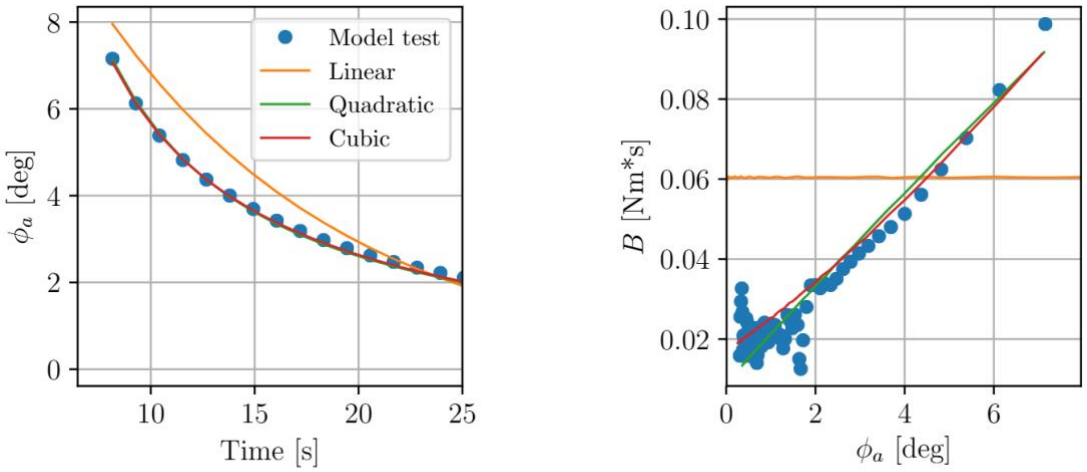

(a) Amplitude decrements. (b) Dampings.

Figure 4.2. Roll decay model test, linear-, quadratic-, and cubic-model.

4.2 Manoeuvring

The wPCC test case Fig. 4.3 is a ship that was designed for wind-assisted propulsion system (WAPS) and can alter between a fully sailing mode, and a fully motoring mode, and in between. However, only the motoring mode was considered in this project. Because of the WAPS, the wPCC design differs slightly from conventional motoring cargo ship designs. The wPCC has two very large rudders, two to three times larger than needed for a conventional ship. System identification was conducted on data from free running model tests with the wPCC.

Figure 4.3. wPCC tested at RISE SSPA Maritime center. Copyright 2020 by RISE.

The wPCC model test data was split into training-, validation-, and testing-sets as shown in Fig. 4.4. The model structure was established by identifying various competing mathematical model structures on the training set and evaluating their accuracy on the validation set. The best performing model was retrained on all the data from the training and validation sets. The accuracy of this final model was evaluated with the test set,

predicting the turning circle test as shown in Fig. 4.5. The final model could estimate the turning circle tests with less than 5% deviation.

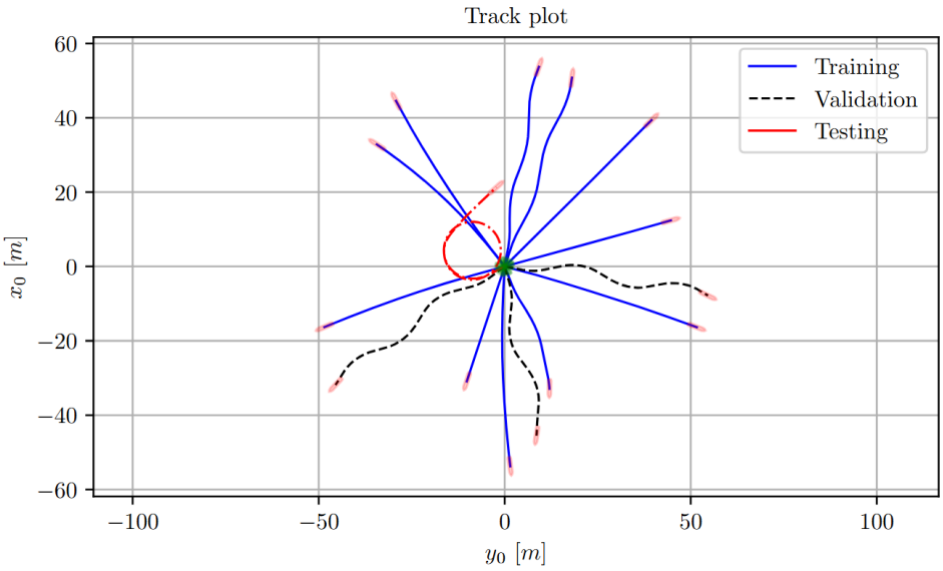

Figure 4.4. wPCC training, validation and testing datasets.

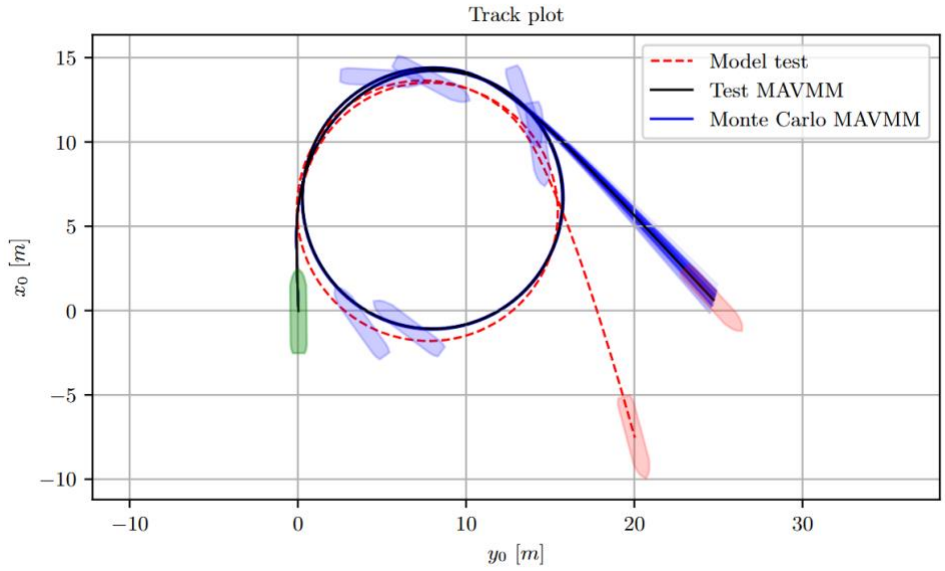

Figure 4.5. Turning circle test case for wPCC, track plots from model test and simulation.

However, it was found that the identified model was physically incorrect, despite yielding good results. Therefore, a physics-informed (PI) model was proposed, incorporating a semi-empirical rudder model. Figure 4.6 compares the forces from the PI model and the original physics-uninformed (PU) model. The identification of the PU model resulted in an incorrect decomposition between the hull yawing moment N_H and the rudder yawing moment N_R due to multicollinearity, as discussed in the introduction of this report. In contrast, the PI model correctly decomposed the rudder and hull forces. Additionally, the decomposition between drift-dependent hull forces $N_H(v)$ and yaw rate-dependent hull forces $N_H(r)$ was more accurate in the PI model compared to the PU model, as shown in Fig. 4.7.

System identification was also conducted on data from captive tests with another test case called Optiwise. This test case involved an ordinary VLCC tanker but with a larger rudder size adopted for WAPS. Significant effort was made to develop an accurate prediction model for the rudder forces. Based on the MMG original rudder model (Yasukawa and Yoshimura, 2015), an enhanced quadratic model was proposed. Figure 4.8 shows a comparison between the rudder forces measured during the Optiwise tests and the predictions from both the MMG original and the enhanced quadratic models. Some states were also calculated using CFD in the state VCTs. There was good agreement between the measured and predicted rudder forces.

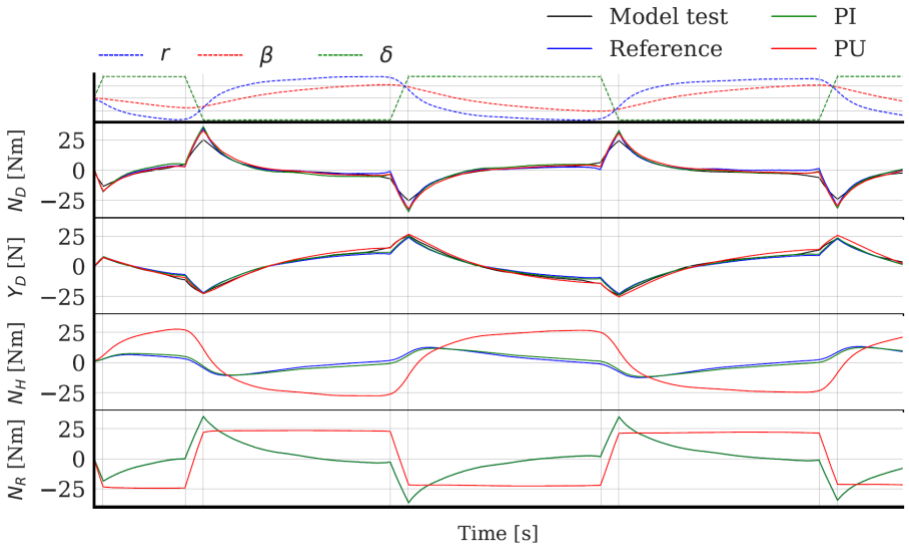

Figure 4.6. Estimations of forces during a zigzag10/10 model test compared with model predictions.

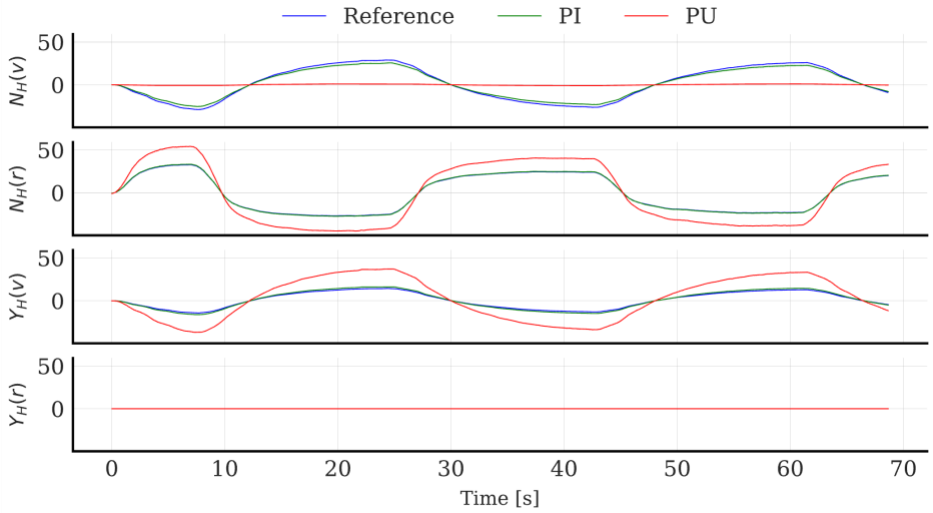

Figure 4.7. Decomposition of hull forces and moments during a zigzag20/20 test for parameters related to drift, yaw rate, and the prediction models.

The identified rudder models could be combined with a hull force prediction model to form a modular manoeuvring model for the entire ship. The total forces from this model were in good agreement with the inverse dynamics forces from the free-running model tests (FRMT), as shown in Fig. 4.9. Additionally, zigzag tests were compared with closed-loop simulations using the developed models, as shown in Fig.4.10. The experiments and

simulations were in good agreement for the zigzag 20/20 test, though there was slightly less agreement for the 10/10 test.

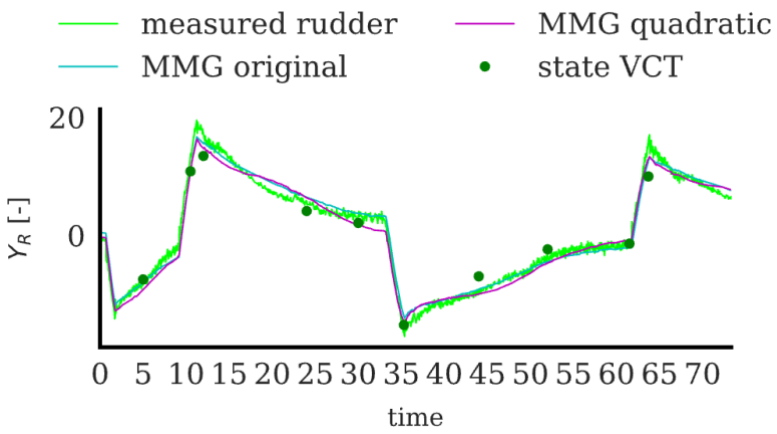

Figure 4.8. Rudder forces during a zigzag test vs predictions with the MMG models.

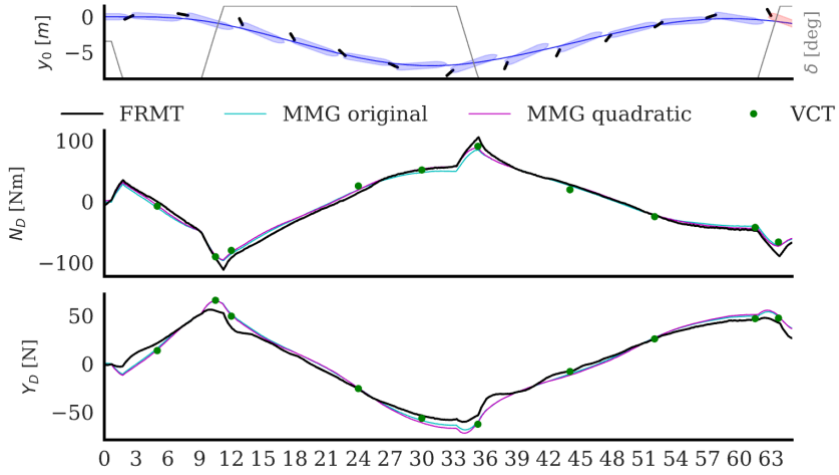

Figure 4.9. Inverse dynamics forces during zigzag tests vs predictions with the MMG models.

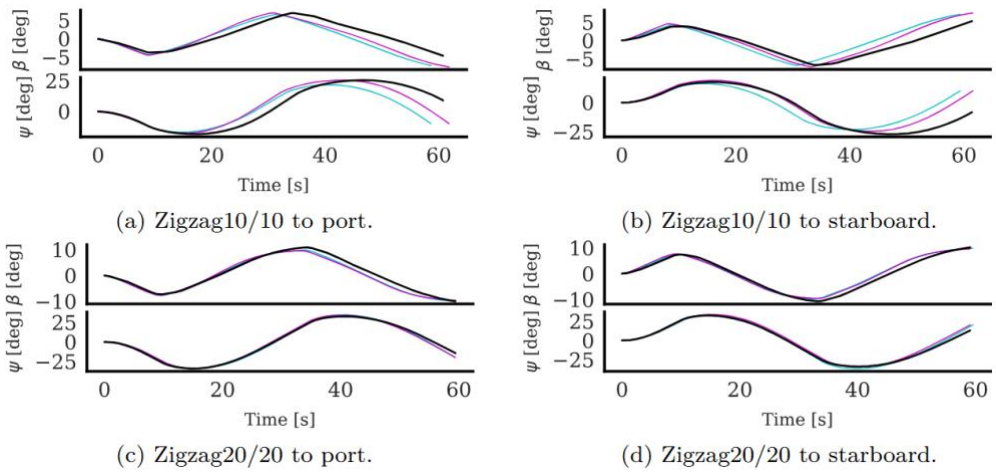

Figure 4.10. Comparison of zigzag tests between Optiwise experiments (black) and simulations with the MMG original (cyan) and MMG quadratic (purple).

5 Results for shipping energy efficiency

In modern ships, captains can issue a command from the ship bridge directly into the engine through the throttle control, which is a lever or handle with different positions that regulates the amount of fuel injection into the compression-ignition cylinders. The fuel intake controls the engine's speed and load and power outputs. The double-ended ferry command bridge has two throttle levers, one for each engine. Finding optimal control strategy of engines to reduce fuel consumption becomes more difficult. Two case study ships are used to demonstrate the fuel saving by implementing data analytics and ML-enhanced decision support system for assisting ship navigation (Vergara, Alexandersson et al. 2023).

5.1 Case study ships

The first case study is a RoRo passenger ship named Uraniborg of ship length 46 meters, service speed 11.5 knots, and two identical internal combustion engines Caterpillar C32 ACERT V12 with maximum rating 709kW of 1600 rpm. The ferry transits the Øresund, specifically the route Ven-Landskrona in southern Sweden, a route that is approximately 4 nautical miles. A basic sketch of such a double-ended vessel is illustrated in Fig. 5.1. The main engine notations (Engine 1 and Engine 2) will switch their functionalities between stern and bow engines for different trip directions. For the sake of convenience, bow and stern engines are used for the description. Table 5.1 summarizes the most relevant parameters to operate those double-ended ferries.

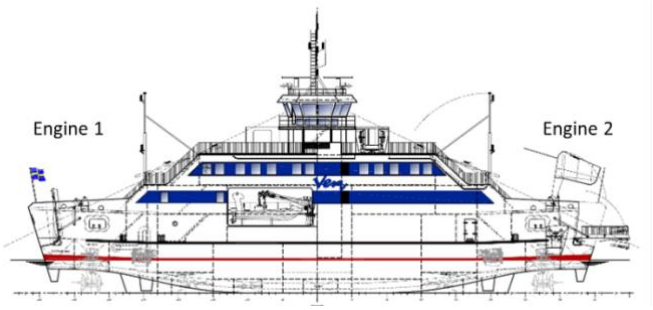

Figure 5.1. General arrangement of a double-ended ferry.

*Table 5.1. Main operational parameters of double-ended ferries. *FCR: Fuel Consumption Rate*

Symbol	Feature	Units	Symbol	Feature	Units
V_g	Speed Over Ground	knots	n_s	Rotation Speed of Stern Engine	rpm
φ_{ship}	Ship Heading	deg	n_b	Rotation Speed of Bow Engine	rpm
L_s	Load of Stern Engine	%	V_{WR}	Relative Wind Speed	m/s
L_b	Load of Bow Engine	%	φ_{WR}	Relative Wind Angle	deg
$\dot{m}_s$	FCR* of Stern Engine	l/h	V_{sc}	Sea Current Speed	m/s
$\dot{m}_b$	FCR* of Bow Engine	l/h	φ_{sc}	Sea Current Angle (North)	deg

The second case study ship is a short sea shipping chemical tanker sailing between ports in European waters, across the Baltic Sea, North Sea and English Channel. Key specifications for the ship are provided in Table 5.2.

Table 5.2: Specifications and Operational Data of the Chemical Tanker

Parameter	**Value**
Length Between Perpendiculars	138.22 m
Breadth	23.76 m
Design Draft	9.27 m
Displacement	25174 m3
Maximum Continuous Rating (MCR)	7200 kW
Service Speed	14 knots
Data Collection Period	Nov 2020 - Mar 2024
Data Frequency	1 sample per minute

The full-scale data from the vessels was down sampled from 1-minute to 10-minute intervals to reduce noise while preserving relevant trends. Some of the example routes are presented in Fig. 5.2 Then, steady-state filters based on first derivative-thresholds were applied to the ship's engine power, engine speed and ship speed, effectively removing transients and manoeuvres. These signals were further smoothed using a second-order Savitzky-Golay filter.

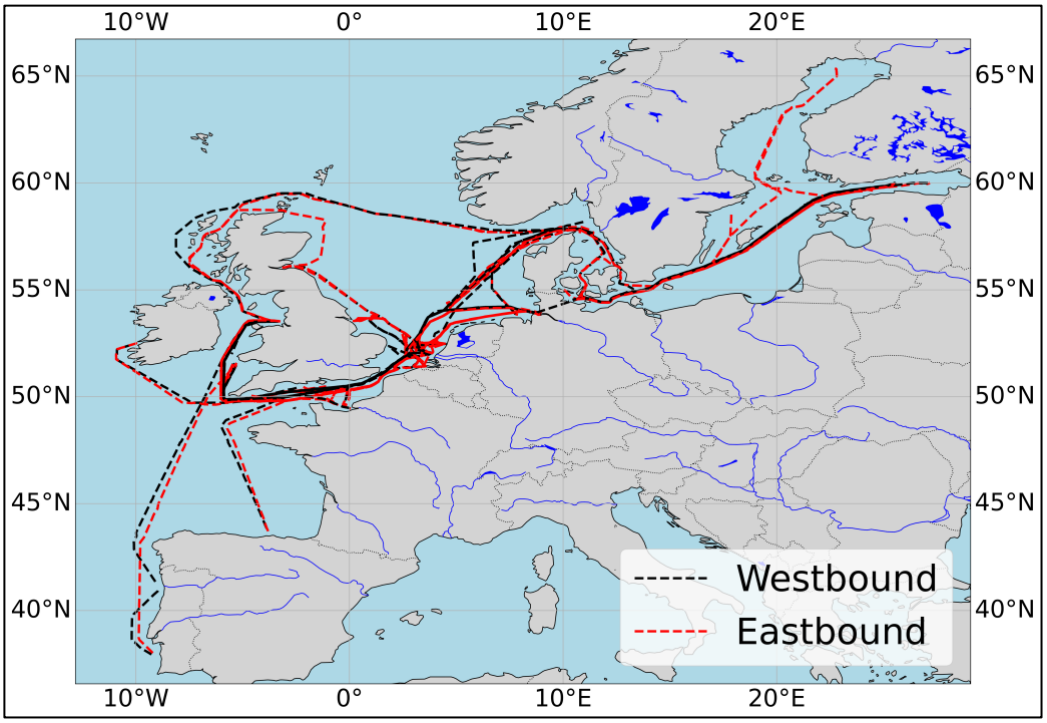

Figure 5.2. Some of the routes from measurements of the second case study ship.

5.2 Data analytics and energy savings of double ended ferry

It is a commuter ferry that goes 18 trips a day in about 30 minutes interval (without too little variations) between both islands. The time series of V_g along a typical trip is shown in

Fig. 5.3, where a one-minute moving average smooth is used to reduce measurement noises.

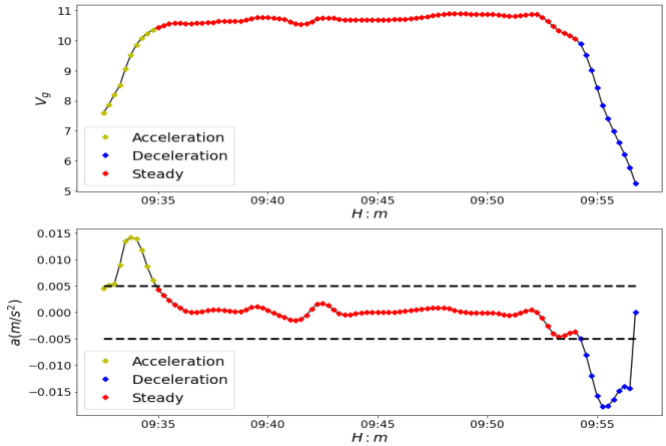

Figure 5.3. Three different sailing stages in terms of speeds (upper plot), and identificaion of steady states by introducing speed acceleration (bottom plot).

Normally, a trip is composed three sailing stages:

- Acceleration, i.e., roughly the first 5 minutes at the start of a trip.
- Steady/Cruising, i.e., the ferry reaches service speed. The derivative of speed, i.e., acceleration, is used to identify the steady states along the trip. For example, the sailing history located between the two dashed lines are considered to be stead state sailing.
- Decceleration, i.e., when the ferry is close to destination and reduces its speed.

Even though ship principles indicate that ship propellers work with highest efficiency when located at the ship stern, how to allocate power distribution between different engines/propellers is still not clear to the operators for those double-ended ferries. In the following, let the power ratio (R_p) be used to describe the power allocation between bow and stern engines as,

$$R_P = \frac{P_{\text{stern}}}{P_{\text{bow}} + P_{\text{stern}}}$$

The average power allocation R_p for each trip is estimated and its distributions are presented in Fig. 5.4. The power allocation is almost equal distributed from 0.5 to 0.9, without significant concentration of putting most of power at the stern engine. In addition, Figure 5.5 presents how the R_p affects total fuel consumption along each trip with fixed ETA. These results show that the lowest total power was observed to occur at a 100% stern power allocation. However, the challenge for the double-ended ferry is that the information of use as much as the stern engine does not guide operators with proper settings for each engine to achieve a given the desired target speed (ETA). Figure 5.55 also indicates that although the mean total fuel consumption decreases with the increments of R_p, there is no guarantee that optimal R_p always occurs at 100% stern allocation due to other influence parameters. Therefore, this study aims at developing onboard DSS to determine the optimal set-points of both bow and stern engines by combining machine learning techniques and optimization algorithms for minimum fuel consumption.

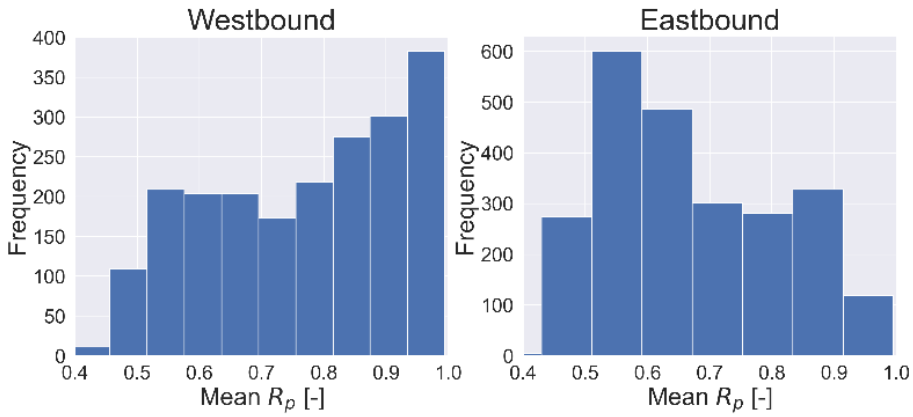

Figure 5.4. Histogram of the distribution of mean engine power allocation ratio for different trips.

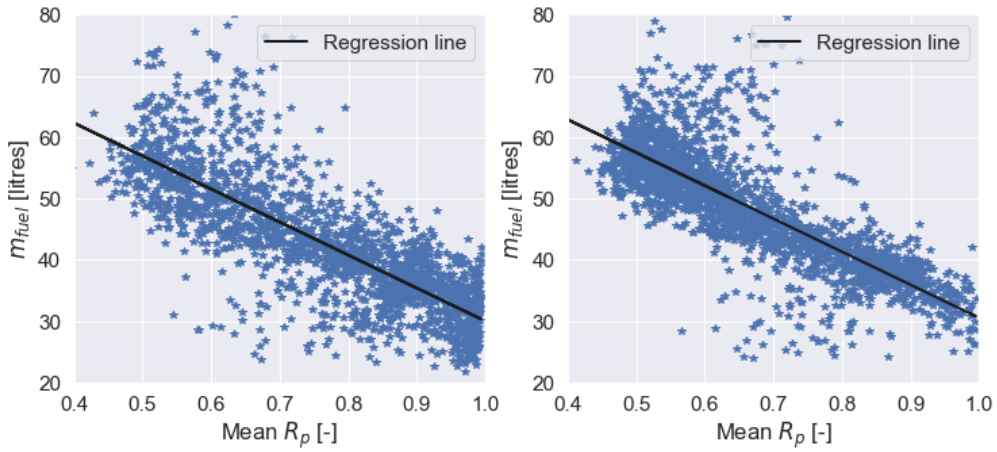

Fig. 5.5, total fuel consumption in terms of mean R_p for each trip of the double-ended ferry

The full-scale tests were conducted between August 19 and August 22 of 2022. The operation was carried out by the ship's captain and the 1st Mate. Before the tests, the captain was instructed to operate the ship by allocating most of the power on the stern thruster according to the DSS guidance. The 1st mate was unaware of the experiment. This set-up simulates the scenarios of DSS stern power allocation (Captain) and the regular arbitrary operation (1st Mate). Figure 5.6 presents the total fuel consumption per trip in terms of power allocation R_p. The observed trend aligns with that from previous data analysis. To have a fair comparison, some trips were filtered out if their mean speed (ETA) differ significantly from normal operations. Figure 5.6 (right) indicates the number of trips filtered out due to their either too high or too low speeds. After filtering 10 trips for each operation modes (i.e., Captain vs 1st Mate) are considered for the analysis. Table 5.4 presents a summary of these results. In average the DSS guided operations of using more stern power (Captain) contribute to up to 18% fuel reduction compared to an arbitrary configuration (1st Mate). The saving might be a bit smaller if their average speeds are the same, but it will not change the results.

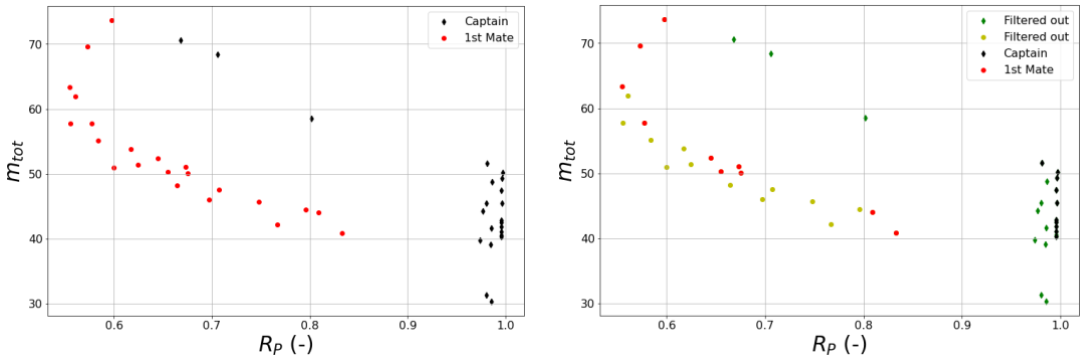

Figure 5.6. Total fuel consumption vs power allocation R_p for different trips, without filtering (left), filtering of trips based on speed/ETA difference (right).

Table 5.3. Summary of the full-scale test results.

Operator	Number of valid trips	$\bar{V}_g$ (knots)	$\bar{M}_{fuel}$ (l)	$\frac{\Delta\bar{M}_{fuel}}{M^0_{fuel}}$
Captain	10	9.4	45.25	-18%
1st Mate	10	9.5	55.31	

5.3 Data-driven ship and engine performance models

Some physical or semi-empirical models are available for practical ship operations, but the physical components and corresponding coefficients inside those models were mainly established from conventional ships. They are often associated with large uncertainties even for those conventional ships, and therefore are capable to model the operation performance of double ended ferries. Given the availability of large volumes of data, machine learning methods become attractive to model a ship's performance more accurately. In this study, the fuel consumption of two engines and the ferry speeds are modelled by the XGBoost method,

$$\dot{m}_s = f_s(n_s,\ L_s,\ n_b,\ L_b,\ W)$$
$$\dot{m}_b = f_b(n_s,\ L_s,\ n_b,\ L_b,\ W)$$
$$V_g = f_v(n_s,\ L_s,\ n_b,\ L_b,\ \varphi_{ship},\ V_{sc},\ \varphi_{sc},\ V_{wr},\ \varphi_{wr})$$

where W denotes all ocean weather related parameters, and the other parameters are described in Table 5.2, and they are chosen as the features of those models because they are acting as either the control variables or constraints of the decision-making system. Before such data-driven ship performance models integrated into the proposed DSS here, the model accuracy was assessed as in Fig. 5.7, which shows good predictions of the two voyages with the measured data.

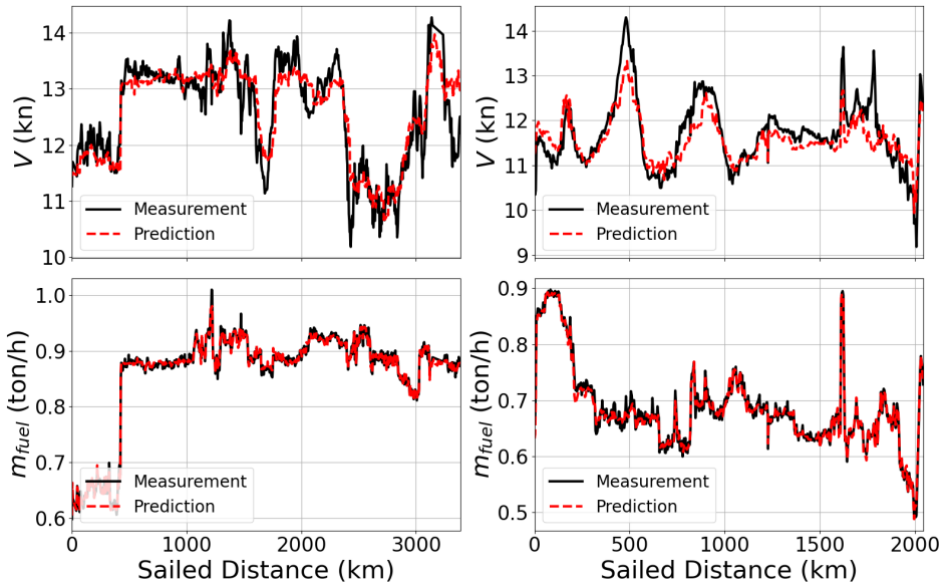

Figure 5.7. Comparison of predicted and measured results for two test voyages: one across the Baltic Sea and North Sea (left), and one across the North Sea and English Channel (right).

Overall, the XGBoost models demonstrate a good ability to predict m_fuel, with predictions closely matching actual measurements across the example voyages, thereby validating the features used and hyperparameters tuned in the model. Predictive accuracy for m_fuel is expected, as the model is informed by key operational variables, such as engine power, which is highly correlated with fuel consumption. However, predicting ship speed V presents larger challenges. While the model successfully captures general trends, it struggles to match the peaks and valleys observed in actual measurements. This discrepancy may be attributed to the high variability of metocean conditions or the exclusion of other operational variables. Nevertheless, the established models accurately capture the overall trend without significant prediction errors, making it sufficient for use in subsequent power allocation optimization to calculate fuel consumption and sailing time.

For voyages across the Baltic Sea and the North Sea, four individual voyages, illustrated in Fig. 5.8 are selected as case studies to validate the proposed engine power allocation method. Detailed voyage information is provided in Table 5.4. Cases 1 and 2 feature relatively long routes, each spanning more than 3000 km and lasting over 140 hours. By contrast, Cases 3 and 4, which take place solely within the Baltic Sea, cover shorter distances of around 1100 km and require approximately 60 hours and 55 hours, respectively.

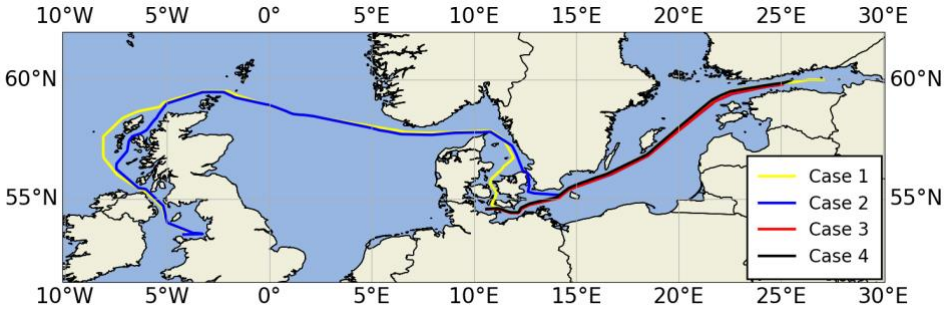

Figure 5.8. The case study voyages across the Baltic Sea and North Sea for power allocation optimization.

Table 5.4. The case study voyages across the Baltic Sea and North Sea.

Case ID	Sailing area	Distance [km]	ETA [hours]	Actual fuel consumption [tons]
1	Baltic and North Sea	3388	145.50	121.6
2	Baltic and North Sea	3089	143.83	86.2
3	Baltic	1118	60.50	26.4
4	Baltic	1153	55.33	26.6

For Case 1 and Case 2, the voyage segmentation results are presented in Fig. 5.9. The power allocation optimization results are shown in Fig. 5.10 for Case 1 and Fig. 5.11 for Case 2, respectively. These figures illustrate the measured engine power and speed during the actual voyages, the optimized power settings for each leg, and the corresponding speeds. The metocean data encountered during the optimized voyage are also presented for a more comprehensive analysis.

(a) (b)

Figure 5.9. Segmented trajectories for voyages across the Baltic Sea and North Sea, showing (a) Case 1 and (b) Case 2.

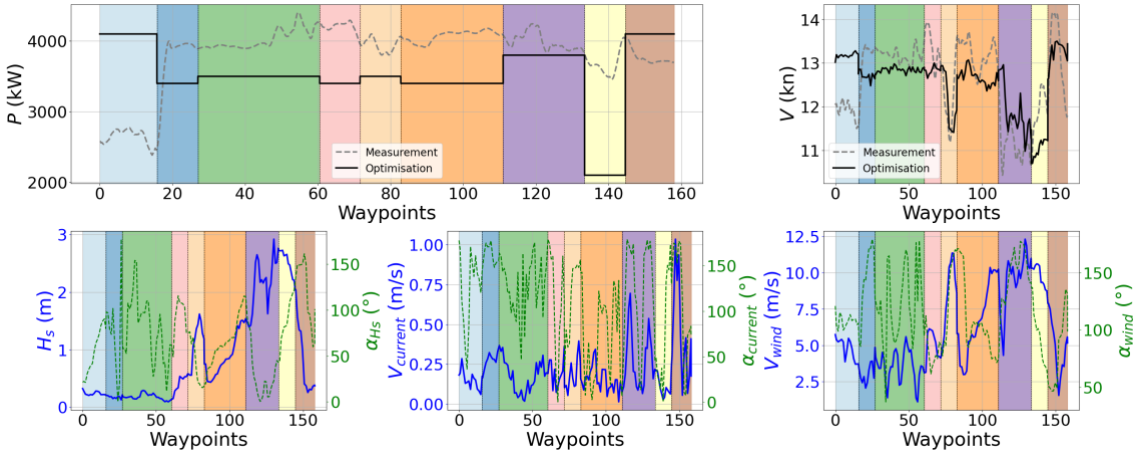

Figure 5.10. Power allocation results for Case 1, including measured and optimized engine power, ship speed, and encountered metocean conditions for each waypoint along the optimized voyage.

As shown in Fig. 5.9 (a), the voyage in Case 1 is segmented into nine legs. The chemical tanker encountered relatively harsh weather conditions, with H_s reaching 3 meters in legs 7 (purple) and 8 (yellow). Under this condition, the power allocation optimization achieved a potential fuel consumption reduction of 8.8 tons, which represents a reduction of 7.2% compared to the actual voyage measurement. As seen in Fig. 5.9, the optimal power allocation strategy prioritizes increased power at the beginning of the voyage when the encountered wave conditions were milder, followed by a significant reduction in power settings during leg 8 to conserve fuel. Although H_s was relatively high, the power setting was still increased in leg 7 due to favorable following wave conditions, which has a smaller wave resistance relative to bow sea and head sea. The actual voyage duration was around

145 hours, while the optimized strategy introduced a minor delay of 17 minutes, well within the acceptable range of 1%.

Similarly, for the voyage in Case 2, as shown in Figs. 5.9 (b) and Fig.5.11, the voyage is segmented into eight legs. Among these segments, legs 2 (blue), 3 (green), 7 (yellow), and 8 (brown) experience peak H_s value exceeding 1.5 meters. In leg 5 (orange), the chemical tanker encountered wind speed V_{wind} exceeding 10 m/s, and current speed $V_{current}$ greater than 1 m/s. The optimal power allocation strategy involved reducing power during legs 3, 5, and 6 (purple), where conditions were least favorable (e.g., high waves and strong head wind). Conversely, power was increased during leg 2 with a following wave and leg 7, which had relatively mild wind conditions. Compared to the actual power settings, this optimized strategy resulted in a fuel consumption reduction of 3.9 tons, which is approximately a 4.5% reduction, with a minor delay of only 5 minutes.

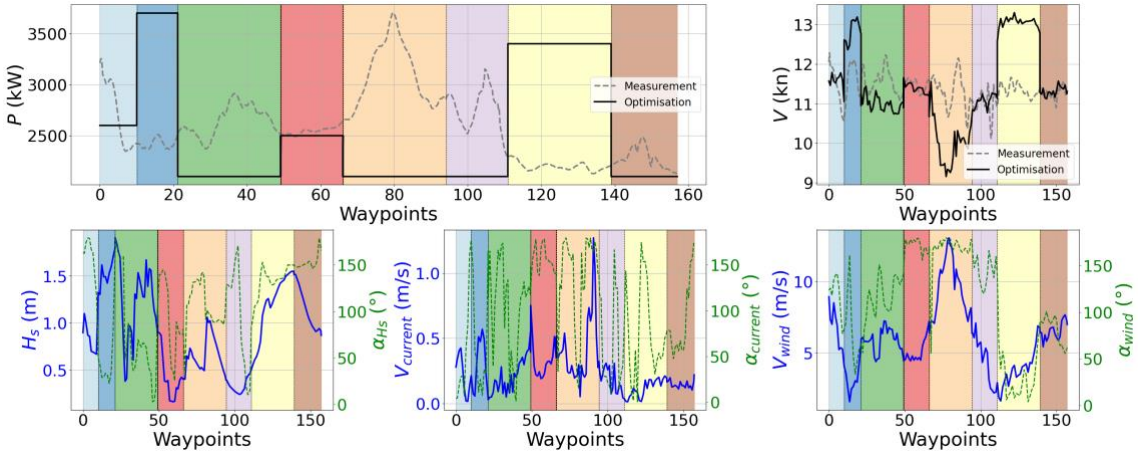

Figure 5.11. Power allocation results for Case 2, including measured and optimized engine power, ship speed, and encountered metocean conditions for each waypoint along the optimized voyage.

The detailed optimized fuel consumption and time delays are presented in Table 5.5. For the shorter Baltic Sea voyages Case 3 and Case 4, the time delays after power allocation optimization also remain under 0.3%, fulfilling the requirement that the total sailing time deviate by no more than 1% from the ETA. Additionally, energy consumption is reduced by 7.1% and 7.3%, respectively. The segmentation times for all case studies are approximately 30 milliseconds. The optimization takes about 90 seconds for Cases 1 and 2, and around 35 seconds for Cases 3 and 4.

Table 5.5. The optimized fuel consumption and time delay of the case study voyages.

Case ID	Time delay [%]	Optimized fuel consumption [tons]	Reduction [%]
1	0.19%	112.8	7.2%
2	0.06%	82.3	4.5%
3	0.28%	24.5	7.1%
4	0.10%	26.5	7.3%

6 Concluding remarks

This project investigated the enhancement of ship manoeuvring models through the integration of prior knowledge embedded in parametric model structures and semi-empirical formulas. The major conclusions are that physically accurate models can be derived from parametric model structures when prior knowledge about ship hydrodynamics and semi-empirical formulas are embedded in the structure, provided that the observed data is correct and informative, as demonstrated with VCT data. It was also concluded that physically accurate models could not be identified from standard manoeuvers, which contained insufficient informative data. However, by adding a semi-empirical rudder model, the identification process was guided towards a more physically accurate model.

Key findings indicate that inverse dynamics regression is an efficient method for parameter identification in parametric models. The proposed quadratic model structure for roll motion demonstrates good generalization, and the new parameter identification method accurately predicts manoeuvring models from standard manoeuvres. However, challenges with multicollinearity and the need for more informative data are highlighted. The study concludes that semi-empirical formulas can guide identification towards more physically correct models, and VCT can provide the necessary data for accurate model identification. The implications of this research suggest that integrating semi-empirical rudder models and utilizing VCT can significantly enhance the accuracy and generalization of ship manoeuvring models, contributing to more reliable and physically accurate simulations in maritime engineering.

For the application of data analytics and machine learning modelling for energy efficiency shipping measures, it is demonstrated that more than 10% energy saving can be easily observed by the doubled ended vessel, by guiding ship operators to put as much as possible the power to the stern engine keeping the same ETA. For the short sea shipping, about 5% fuel savings can be found by the proposed method in this project.

7 Further reading reference

This work has been carried out in the framework of a PhD thesis by Martin Alexandersson. The research project (DEMOPS) has been financed in two different stages (Part I, 2010-2023 and Part II ,2023-2025) by the Swedish Transport Administration operated by Lighthouse. The detailed explanation of the methods and findings from this research project is reported in Martin Alexandersson's PhD thesis (enclosed to this report).

8 References

Abkowitz, M.A., 1964. Ship hydrodynamics - steering and manoeuvrability. Hydro-Aerodyn. Lab. Hydrodyn. Sect. Lyngby Den. Rep. No Hy-5 Lect.

Alexandersson, M., Mao, W. and Ringsberg, J. (2021). Analysis of roll damping model scale data., Journal of ship and offshore structures, Vol. 16 Issue sup 1 p. 85-92.

Alexandersson, M., Mao, W., & Ringsberg, J. W. (2022). System identification of vessel manoeuvring models. Ocean Engineering, 266, 112940

Alexandersson, M., Zhang, D., Mao, W., & Ringsberg, J. W. (2023). A comparison of ship maneuverability models to approximate ship navigation trajectories. Ships and Offshore Structures, 18(4), 550-557.

Alexandersson, M., Mao, W., Ringsberg, J., Kjellberg, M. (2024). System identification of a physics-informed ship model for better predictions in wind conditions. Ocean Engineering, 310, 118613.

Alexandersson, M. (2025). System identification and prediction models in ship dynamics. PhD thesis at Chalmers University of Technology.

Chen, Y., & Mao, W. (2024). An Isochrone-Based Predictive Optimization for Efficient Ship Voyage Planning and Execution. IEEE Transactions on Intelligent Transportation Systems.

Holtrop, J., Mennen, G., 1982. An approximate power prediction method. Int. Shipbuild. Prog. 29 (335), 166–170.

ISO, 2015. Ships and marine technology - Guidelines for the assessment of speed and power performance by analysis of speed trial data, 15016.

ITTC, 2012. Analysis of speed/power trial data, Recommended procedures and

guidelines 7.5-04-01-01.2.

Jinkine, V., Ferdinande, V., 1974. A method for predicting the added resistance of fast cargo ships in head waves. Int. Shipbuild. Prog. 21 (238), 149–167.

Lang, X., Zhang, M., Zhang, C., Ringsberg, J. W., & Mao, W. (2024). Physics-guided metamodel for vertical bending-induced fatigue damage monitoring in container vessels. Ocean Engineering, 312, 119223.

Lang, X., Wu, D., & Mao, W. (2024). Physics-informed machine learning models for ship speed prediction. Expert Systems with Applications, 238, 121877.

Lang, X., Wu, D., & Mao, W. (2022). Comparison of supervised machine learning methods to predict ship propulsion power at sea. Ocean Engineering, 245, 110387.

Nomoto, K., Taguchi, T., Honda, K., Hirano, S., 1957. On the steering qualities of ships. Osaka Univ. Dep. Nav. Archit. Jpn. Publ. Int. Shipbuild. Prog. ISP Vol. 4 No 35 1957 Pp 354-370.

Norrbin, N.H., 1971. Theory and observations on the use of a mathematical model for ship manoeuvring in deep and confined waters. Publ. 68 Swed. State Shipbuild. Exp. Tank Göteb. Swed. Proc. 8th Symp. Nav. Hydrodyn. ONR Pasadena Calif. Pp 807-905.

Strom-Tejsen, J., Yeh, H., Moran, D., 1973. Added resistance in waves. Trans. Soc. Nav. Archit. Mar. Eng. 81, 109–143.

Vergara, D., Alexandersson, M., Lang, X., & Mao W. (2023). A machine learning based Bayesian decision support system for efficient navigation of double-ended ferries. Journal of Ocean Engineering and Science.

Wang, H., Mao, W. and Eriksson, L. (2019). A Three-Dimensional Dijkstra's algorithm for multi-objective ship voyage optimization. Ocean engineering, Vol.186, No. 106131.

Yasukawa, H., Yoshimura, Y., 2015. Introduction of MMG standard method for ship maneuvering predictions. J. Mar. Sci. Technol. 20, 37–52. https://doi.org/10.1007/s00773-014-0293-y

Yoon, H.K., Rhee, K.P., 2003. Identification of hydrodynamic coefficients in ship maneuvering equations of motion by Estimation-Before-Modeling technique. Ocean Eng. 30, 2379–2404. https://doi.org/10.1016/S0029-8018(03)00106-9